Phase transformations in thermally cycled Cu/ZrW_2O_8 composites investigated by synchrotron x-ray diffraction

2002 J. Phys.: Condens. Matter 14 365

(http://iopscience.iop.org/0953-8984/14/3/307)

INSTITUTE OF PHYSICS PUBLISHING JOURNAL OF PHYSICS: CONDENSED MATTER

J. Phys.: Condens. Matter **14** (2002) 365–375 PII: S0953-8984(02)27075-7

Phase transformations in thermally cycled Cu/ZrW_2O_8 composites investigated by synchrotron x-ray diffraction

S Yilmaz

Department of Mechanical Engineering, Istanbul Technical University, Istanbul, Turkey

E-mail: safyil@mkn.itu.edu.tr

Received 24 July 2001, in final form 7 November 2001
Published 21 December 2001
Online at stacks.iop.org/JPhysCM/14/365

Abstract

A Cu/ZrW_2O_8 metal matrix composite was thermally cycled between 298 and 591 K while being subjected to x-ray diffraction in transmission using high-intensity synchrotron radiation. The reversible allotropic phase transformations of ZrW_2O_8 between its two low-pressure phases and its high-pressure phase were observed within the composite bulk as a function of temperature. This observation gives experimental proof of the existence of the reversible pressure-induced phase transformation, which had been inferred indirectly from dilatometry in a previous investigation and assigned to the large thermal mismatch stresses in the composite. The volume fraction of each ZrW_2O_8 compound was determined from the measured diffracted intensity, and the thermal expansion behaviour of the composite was then calculated. Good agreement was found with the experimental dilatometric curve reported in a recent investigation.

1. Introduction

Metal matrix composites (MMCs) consisting of metallic matrix with high thermal conductivity and a ceramic reinforcement with low thermal expansion provide exceptional freedom in tailoring these two properties to practical applications. Optics, space structures, metrology and electronics are some example fields for such kinds of application. Cu/ZrW_2O_8 MMCs are powerful candidates for applications requiring a material having optimum heat conductivity and dimensional thermal stability [1]. As reported in [2–10], ZrW_2O_8 has a negative coefficient of thermal expansion (CTE). This unusual thermal expansion behaviour is due to a steric contraction of the open network of polyhedra by back-and-forth tilting of polyhedra, which outweighs the usual chemical bond thermal expansion. The CTE of ZrW_2O_8 is isotropic and has a large magnitude ($\alpha = -12 \times 10^{-6}$ to -5×10^{-6} K^{-1}) over a very large temperature range (0–1050 K). Furthermore, ZrW_2O has three polymorphs [10]: two cubic phases at ambient

pressure (α-ZrW_2O_8 below 423 K and β-ZrW_2O_8 above 423 K) and one orthorhombic phase at high pressure (γ-ZrW_2O_8), with a CTE close to zero.

Holzer and Dunand [1] recently prepared MMCs consisting of a high-conductivity copper matrix containing ZrW_2O_8 particles with negative CTE. Using dilatometry, they measured the thermal expansion of these composites and found that it was much higher than predicted from thermo-elastic theory. This discrepancy was attributed to the presence of the high-pressure γ-phase produced during processing and subsequent cooling of the sample: on heating in the dilatometer, transformation of γ-ZrW_2O_8 to one of the low-pressure α- or β-phases is accompanied by polymorphic volume expansion of 5.0% [9]. On subsequent cooling in the dilatometer, the thermal expansion mismatch between the copper matrix and the ceramic particles is large enough to produce a hydrostatic stress in the ceramic of the same magnitude as that observed to induce the high-pressure transformation in loose ZrW_2O_8 powders (occurring over a hydrostatic pressure range of 200–300 MPa [9]). Holzer and Dunand [1] thus explained that the large dilatometric expansion on heating and contraction on cooling matched those expected from the phase transformation. However, the evidence for this reversible pressure-induced transformation produced in the composite during fabrication and subsequent thermal cycling was only indirect.

Diffraction methods are useful for *in situ*, real-time observation of phase transformations, as the volume fraction of each phase can be inferred by its diffracted intensity. Synchrotron x-ray diffraction offers higher penetration depths than laboratory x-ray (thus allowing true bulk measurement) and shorter data collection times than neutron diffraction. Synchrotron x-ray diffraction is often used to study pressure-induced phase transformations in materials confined in pressure cells (e.g. [11, 12]) but less frequently for temperature-induced phase transformations in samples heated at ambient pressure (e.g. [13–15]). This paper reports on synchrotron x-ray diffraction experiments on thermally cycled Cu–ZrW_2O_8 composites.

2. Experimental procedures

In this study, the same composite material as investigated by Holzer and Dunand [1] was used. The sample consisted of a continuous copper matrix with a volume fraction of 60% ZrW_2O_8. The composite was prepared by hot isostatic pressing (HIP) of copper-coated ceramic particulate with average size 53 μm (more details can be found in [1]). The specimen used in the present experiments was rectangular with $1.7 \times 4.5 \times 12.5$ mm^3 dimensions, had smooth surfaces and had been cycled four times between 293 and 593 K three months before the present experiment.

The x-ray diffraction experiment took place at the bending magnet beam line 5BM-D of the Advanced Photon Source (Argonne National Laboratories, IL, USA). As shown in figure 1, the centre of the specimen was irradiated with a monochromatic, parallel beam of 62 keV x-rays (corresponding to a wavelength of $\lambda = 0.20$ Å) with approximate dimensions 0.25×0.25 mm^2 impinging in the centre of, and perpendicular to, one of the 4.5×12.5 mm^2 faces of the specimen. Thus, the volume under investigation was 0.11 mm^3 and contained about 1000 ceramic particles. The transmitted beam of high intensity was absorbed at a beam-stop while the diffraction patterns consisting of concentric rings belonging to each phase were recorded with a two-dimensional charge-coupled device (CCD) camera placed 551 mm away from the sample. The CCD camera (from MAR, IL, USA) consists of an orthogonal array of square pixels (each 64×64 μm^2 in size and with 16-bit intensity reading) covering a circular area 132 mm in diameter. Two successive exposures of 300 s were combined into a single diffraction pattern after elimination of spotlike, random signals caused by background radiation, using the software package MRCCD (version 3.19i by MAR, IL, USA).

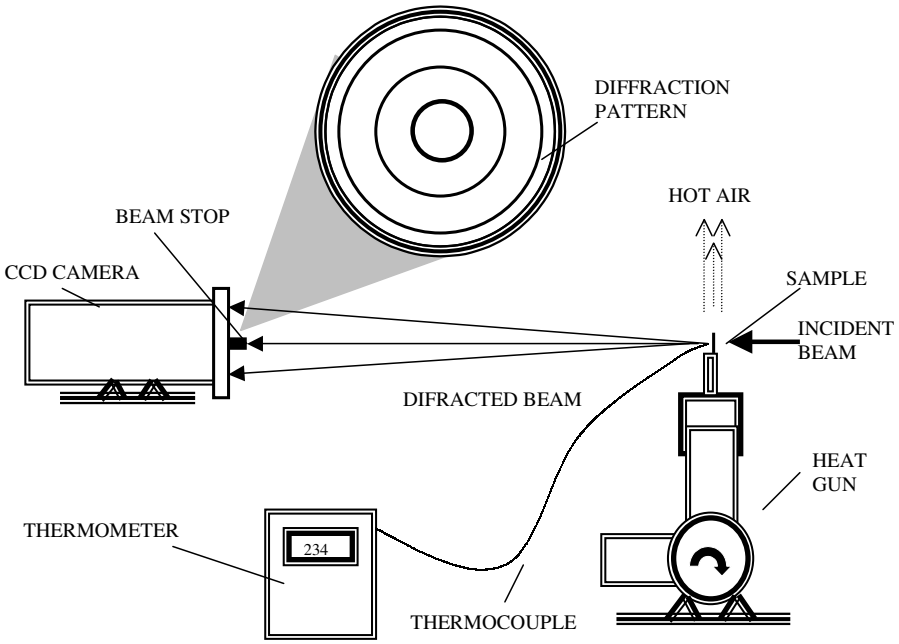

Figure 1. Schematic representation of transmission synchrotron x-ray diffraction test set-up.

The specimen was heated in air from 298 to 591 K and cooled back to 298 K using a heat-gun. The temperature, as measured with a small K-type thermocouple in contact with the specimen, was stabilized within ± 2 K at intervals of about 50 K for a few minutes, followed by diffraction measurement of 10 min duration.

3. Data analysis

Figure 2 shows a diffraction pattern with the most intense ceramic diffraction rings and the Cu(111) ring marked. Each diffraction ring has a certain thickness determined by the diffraction angle, the beam width and the sample thickness. The volume fractions of the phases of ZrW_2O_8 were calculated from the ring intensities as explained in the following.

The approximate centre of the diffraction pattern was first determined and an average radius R was measured for each ring. An annulus ranging from radius $R - \Delta R$ to radius $R + \Delta R$ was chosen for each ring, so as to cover the ring without overlapping with neighbouring rings which are not evaluated. The intensity of each pixel within that annulus was read (using a custom program written in Visual Basic) and added to yield a total ring intensity. A control annulus with the same total pixel number was chosen in the immediate vicinity of the investigated ring, such that it did not overlap with the ring. The total intensity of that control annulus, corresponding to the background intensity, was subtracted from the total ring intensity to obtain the net ring intensity.

Even if the volume fraction of a given phase is constant, its net ring intensities can vary due to variation in the photon energy or total flux of the primary x-ray beam. Because the copper volume fraction does not vary with temperature, the net intensity of the Cu(111) ring can be used as an internal standard. For each exposure at temperature T, a normalization factor N was thus calculated as the ratio of the net Cu(111) intensity $I_{Cu}(T)$ at that temperature and

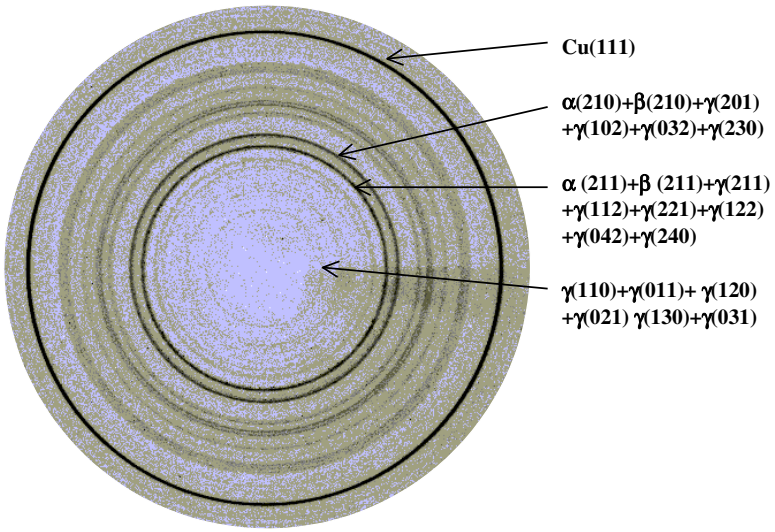

Figure 2. X-ray diffraction pattern of Cu–ZrW_2O_8 composite at room temperature before heating. Main diffraction rings used in the analysis are marked.

(This figure is in colour only in the electronic version)

the net intensity $I_{Cu}(T_0)$ at room temperature ($T_0 = 298$ K). The ceramic normalized ring intensity I_N at temperature T was then calculated as the ratio of the net ring intensity $I_{Cer}(T)$ at that temperature and the initial net intensity $I_{Cer}(T_0)$ at room temperature, divided by the normalization factor N to take into account any fluctuation in the primary beam flux or energy.

$$I_N(T) = \frac{1}{N}\frac{I_{Cer}(T)}{I_{Cer}(T_0)}. \tag{1}$$

If the ring under consideration belongs only to a single ceramic phase, the volume fraction was assumed to be linearly proportional to its normalized intensity I_N. If however the ring consists of overlapping individual rings from two or three phases, the total normalized intensity I_N was assumed to follow a simple rule of mixtures (ROM) of each phase present:

$$V_{f,\alpha} I_{N,\alpha} + V_{f,\beta} I_{N,\beta} + V_{f\gamma} I_{N,\gamma} = I_N \tag{2}$$

where $I_{N,\alpha}$, $I_{N,\beta}$ and $I_{N,\gamma}$ are respectively the normalized intensities of the pure α, β and γ phases (assumed to be temperature independent) and $V_{f,\alpha}$, $V_{f,\beta}$ and $V_{f,\gamma}$ are the temperature-dependent volume fractions of each ceramic phase with respect to total ceramic volume:

$$V_{f,\alpha} + V_{f,\beta} + V_{f,\gamma} = 1. \tag{3}$$

The procedure given with equation (1) relies on the same temperature dependence of Debye–Waller factors of pure copper and ZrW_2O_8 and the validity of this assumption is discussed below.

4. Result

As listed in table 1, the lattice parameters of α-, β- and γ-ZrW_2O_8 are very close to each other, except for the b dimension of the unit cell of γ-ZrW_2O_8. Therefore, most diffraction rings overlap for these phases and/or are too weak to be easily detected. One exception is the combined $\gamma(110) + \gamma(011) + \gamma(120) + \gamma(021) + \gamma(130) + \gamma(031)$ ring

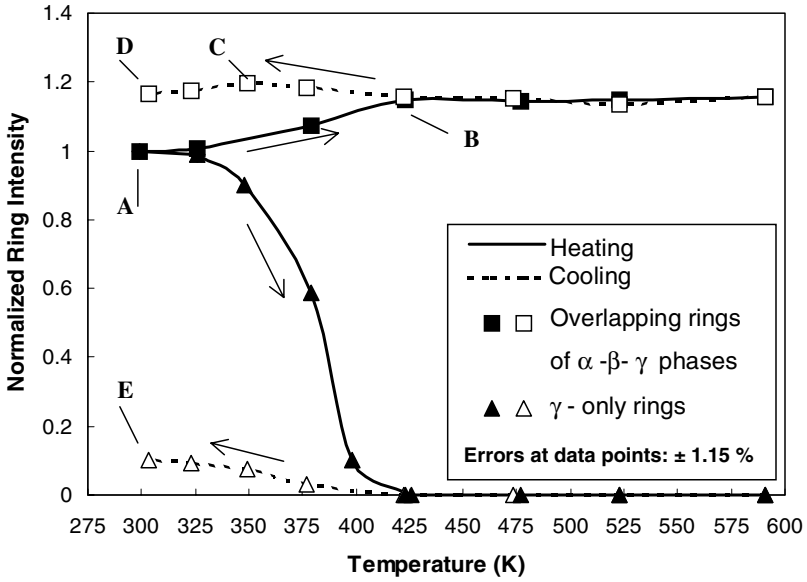

Figure 3. Measured normalized diffraction ring intensities of Cu–ZrW_2O_8 as a function of temperature upon heating and subsequent cooling.

Table 1. Lattice parameters of the α-, β- and γ-phases of ZrW_2O_8 at ambient pressure.

Phase	*a* (Å)	*b* (Å)	*c* (Å)	*T* K	Ref.
α	9.157	9.157	9.157	293	[4]
α	9.142	9.142	9.142	423	[4]
β	9.137	9.137	9.137	483	[4]
γ	9.070	27.030	8.917	301	[7]

(figure 2), whose normalized intensity is shown in figure 3 as a function of temperature and is assumed to be directly proportional to the γ-phase volume fraction. Figure 3 shows that, as hypothesized in [1], the composite contained a substantial amount of the γ-phase at room temperature because of the thermal mismatch stresses produced on cooling. Figure 3 also shows unequivocally that, on heating, the ring-normalized intensity of the γ-phase (and thus its volume fraction) decreases to near zero in the temperature interval 323–423 K, in general agreement with the temperature range of 388 ± 8 K for $\gamma \rightarrow \alpha$ transformation of unconstrained powders of γ-ZrW_2O_8 [9]. During the cooling part of the thermal cycle, figure 3 indicates that some γ-phase appears in the temperature interval 423–298 K. This reversible transformation of γ-ZrW_2O_8 was also predicted by Holzer and Dunand [1] based on dilatometric measurements of the composites.

To study the temperature dependence of the $\alpha + \beta$ volume fraction, the two most intense ceramic rings were chosen (figure 2). Each ring consists of three overlapping rings belonging to each of the phases: six of $\alpha(210)$, $\beta(210)$ and $\gamma(201)$, $\gamma(102)$, $\gamma(032)$, $\gamma(230)$ for the inner ring, and three of $\alpha(211)$, $\beta(211)$ and $\gamma(211)$, $\gamma(112)$, $\gamma(221)$, $\gamma(122)$, $\gamma(042)$, $\gamma(240)$ for the outer ring in figure 2. Figure 3 shows the combined normalized intensity of this double ring (consisting of the individual sub-rings above) as a function of temperature. Above 428 K, the γ-phase volume fraction is zero (the $\gamma(110) + \gamma(011) + \gamma(120) + \gamma(021) +$

$\gamma(130) + \gamma(031)$ ring completely disappeared), and the α-phase is unstable, so it can be concluded that all of the ceramic phase consists of the β-ZrW_2O_8. As expected, the normalized intensity of the double ring is constant above 423 K (figure 3). Upon cooling below this temperature (point B) at which the $\beta \rightarrow \alpha$ transformation is expected, the double-ring normalized intensity increases slightly, indicating that the normalized intensity from the $\alpha(210) + \alpha(211)$ sub-rings is slightly greater than that of the $\beta(210) + \beta(211)$ sub-rings. The small intensity decrease on further cooling to room temperature between point C and point D can be explained by assuming that the $\beta \rightarrow \alpha$ transformation is completed at point C and the $\alpha \rightarrow \gamma$ transformation occurs, with the normalized intensity of $\gamma(201)$, $\gamma(102)$, $\gamma(032)$, $\gamma(230)$, $\gamma(211)$, $\gamma(112)$, $\gamma(221)$, $\gamma(122)$, $\gamma(042)$, $\gamma(240)$ sub-rings being lower than that of the $\alpha(210) + \alpha(211)$ sub-rings. At the end of the cycle (point D), the α-phase fraction is much higher than at the beginning (point A). As reported by Holzer and Dunand [1], macroscopic shrinkage of composite samples took place at room temperature over a time frame of about 48 h after the dilatometric experiment, explained as a sluggish $\alpha \rightarrow \gamma$ transformation produced by internal mismatch stresses. This slow transformation at room temperature could not be studied by x-ray synchrotron diffraction due to experimental time constraints.

While two successive exposures of a single diffraction pattern were also used for data acquisition of the CCD camera through software package MRCCD (version 3.19i by MAR, IL, USA), the error magnitude in the intensity readings is needed for error assumption of the results. The same temperature results belonging to the whole ceramic phase consisting of β-ZrW_2O_8 above 423 K in figure 3 can be used for prediction of error occurring in the data of an exposure. For this purpose, the ratios of the net ring intensity of ceramic ($I_{Cer}(T)$) and the net intensity of copper ($I_{Cu}(T)$) at the same temperatures (T) of the heating and cooling part of the thermal cycle above 423 K were compared. The errors of $I_{Cer}(T)/I_{Cu}(T)$ ratios were found as maximum $\pm 0.57\%$ (minimum $\pm 0.32\%$). Therefore the error propagated for normalized intensity calculated by equation (1) was assumed to be $\pm 1.15\%$ for data given in figure 3. In order to see the temperature dependence of x-ray intensities, the ratios of $I_{Cer}(T)/I_{Cu}(T)$ at all temperatures above 423 K were also compared. It was seen that those ratios were distributed randomly and did not show a regular trend with respect to varying temperature. This means that the error resulting from the assumption of the same temperature dependence of Debye–Waller factors of pure copper and ZrW_2O_8 in equation (1) is less than the errors of other effects and its error contributions are included in the errors of $I_{Cer}(T)/I_{Cu}(T)$ ratios (predicted above as $\pm 0.57\%$).

The volume fractions of α-, β- and γ-phase can be calculated for each temperature using equations (2) and (3) and three special values of normalized ring intensities at different temperatures. First, the normalized intensity of pure β-phase was determined as $I_{N,\beta} = 1.1481$, the average of the normalized intensities of the double rings between 473 to 591 K (figure 3), where the α-phase and γ-phase volume fractions are zero. Second, the normalized intensity of the pure α-phase was taken as $I_{N,\alpha} = 1.1955$ at 349 K on cooling (point C in figure 3), at a temperature where the β-phase volume fraction is expected to be zero and neglecting the small volume fraction of the γ-phase. The theoretical intensities of γ rings were calculated [9, 16]. The magnitude of theoretical intensity of $\gamma(201) + \gamma(102) + \gamma(032) + \gamma(230) + \gamma(211) + \gamma(112) + \gamma(221) + \gamma(122) + \gamma(042) + \gamma(240)$ sub-rings is 6.08 times greater than the theoretical intensity of $\gamma(110) + \gamma(011) + \gamma(120) + \gamma(021) + \gamma(130) + \gamma(031)$ rings (figure 2). Finally, using equations (2) and (3) at room temperature at point A in figure 3, and considering the errors given above, the initial volume fraction of γ-phase was found to be $V_{f,\gamma} = 0.207 \pm 0.014$ (at point A) and the normalized intensity of pure γ-phase was found to be $I_{N,\gamma} = 0.2526 \pm 0.0189$ for $\gamma(201) + \gamma(102) + \gamma(032) + \gamma(230) + \gamma(211) + \gamma(112) + \gamma(221) + \gamma(122) + \gamma(042) + \gamma(240)$ sub-rings.

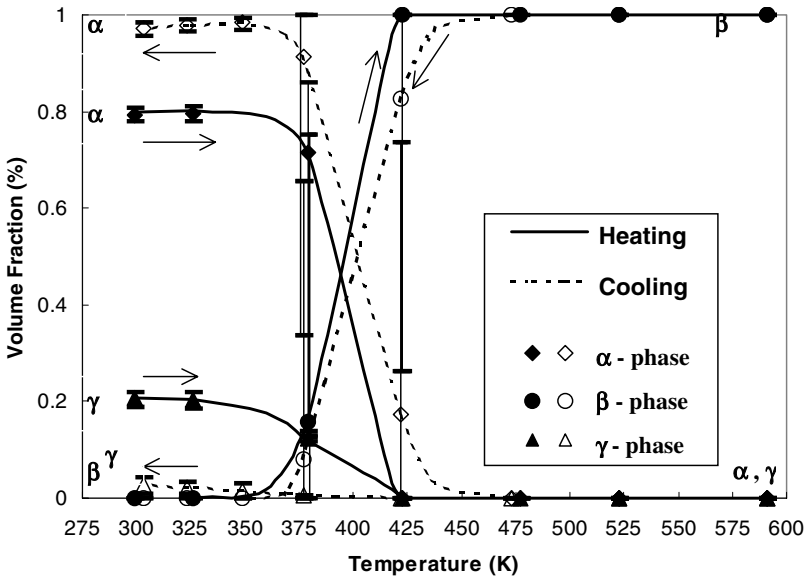

Figure 4. Temperature dependence of the volume fractions of the three ceramic polymorphic compounds in Cu–ZrW_2O_8 composite upon heating and subsequent cooling. The error bars on data points are also marked.

This value of initial volume fraction of γ-phase is in general agreement with values of 29 and 13% found by Holzer and Dunand [1] through the calculations based on overall residual strain measurements after the first and second cycle, respectively, of the as-fabricated Cu/ZrW_2O_8 composite. In the present study, finding a value lower than the volume fraction of 29% is expectable since the as-received material includes more γ-phase due to the pressure effect of the HIP process. Finding a value higher than the volume fraction of 13% is also acceptable because the porosity of composite affects the overall residual strain of the material.

5. Discussion

The volume fractions of the α-, β- and γ-phases calculated according to the above procedure are plotted in figure 4 as a function of temperature. As expected from figure 3, a mixture of α- and γ-phases is present at room temperature at the beginning and end of the cycle, and only β-phase occurs above 423 K. However, at intermediate temperatures, the transformation history is more complex. Owing to the very close magnitudes of normalized intensities of the α- and β-phases, the error bars for calculated volume fractions of these phases are broad when both α- and β-phases exist at intermediate temperatures (figure 4). However the general trends of lines in figure 4 indicate the following.

On heating, all three phases can be present at 378 K, indicating that the α- and γ-phases have partially transformed into the β-phase. This is in contrast to observations that unconstrained α-ZrW_2O_8 powders exhibit a sharp $\alpha \rightarrow \beta$ transformation at 428 K [4] and that unconstrained γ-ZrW_2O_8 powders transform to the α-ZrW_2O_8 over a narrow range of 388 $\pm$ 8 K at ambient pressure [9]. Possible reasons for this low-temperature onset of transformation to the β-phase in the composite include the presence of internal stresses (which may affect the kinetics and thermodynamics of both transformations) and minor contamination

of the ceramic particles by diffusion of copper from the matrix, as observed in [17] (thus shifting the transformation temperatures).

On cooling, figure 4 shows that the $\beta \rightarrow \alpha$ transformation occurs over a broad range of temperature (from above 423 K to below 373K), shifted to higher temperatures as compared with heating where no α-phase exists at 423 K, and much broader than the sharp $\beta \rightarrow \alpha$ transformation at 428 K reported for unconstrained powders [4]. Below 373 K, the $\alpha \rightarrow \gamma$ transformation takes place, conforming the hypothesis of Hulzer and Dunand [1] that compressive thermal mismatch stresses can trigger the formation of the high-pressure phase. A recent neutron diffraction study of unconstrained α-ZrW_2O_8 [9] showed that the transformation to the γ-phase starts at a hydrostatic compressive pressure of 200 MPa and that the γ-phase volume fraction increases linearly to 100% over a relatively broad range of 100 MPa. As shown by Hulzer and Dunand [1], compressive hydrostatic stresses of this magnitude are indeed expected to build up within the ceramic upon cooling of the composite, given very large CTE mismatch between matrix and particle.

Once the ceramic phase volume fractions are known (figure 4) the average thermal expansion of the composite can be calculated and compared with the experimental thermal expansion curves reported by Hulzer and Dunand [1]. A ROM which represents the lowermost bound is

$$\alpha_{\mathrm{ROM}} = V_{\mathrm{fm}}\alpha_{\mathrm{m}} + V_{\mathrm{fp}}\alpha_{\mathrm{p}} \tag{4}$$

where V_{f} is volume fraction, α denotes CTE value and subscripts m and p denote matrix and particle, respectively. Turner's expression [18] based on elastic interactions between matrix and particle gives an upper bound for the composite CTE as

$$\alpha_T = \frac{V_{\mathrm{fm}}\alpha_{\mathrm{m}}K_{\mathrm{m}} + V_{\mathrm{fp}}\alpha_{\mathrm{p}}K_{\mathrm{p}}}{V_{\mathrm{fm}}K_{\mathrm{m}} + V_{\mathrm{fp}}K_{\mathrm{p}}} \tag{5}$$

where V_{f} is the volume fraction, α is the CTE, K is the bulk modulus and the subscripts m and p are for composite, matrix and particle, respectively.

For the effective CTE value of the ceramic phase, a simple rule of mixtures was used:

$$\alpha_{\mathrm{p}} = V_{\mathrm{f}\alpha}\alpha_\alpha + V_{\mathrm{f}\beta}\alpha_\beta + V_{\mathrm{f}\gamma}\alpha_\gamma - \frac{0.05}{3}\frac{\Delta V_\gamma}{\Delta T} \tag{6}$$

where $\Delta V/\Delta T$ is the $(\alpha, \beta) \leftrightarrow \gamma$ polymorphic volume change and $\Delta V_\gamma/\Delta T$ is the change of γ-phase volume fraction over the temperature interval ΔT.

Figure 5 shows the predicted thermal strain calculated from equations (4) and (5) with the volume fractions given in figure 4 and the materials parameters of table 2. Also shown in figure 5 is the thermal strain of the same composite as measured by dilatometry by Hulzer and Dunand [1]. The large thermal expansion on heating observed by dilatometry is accurately predicted and can thus be attributed to the volume expansion associated with the $\gamma \rightarrow (\alpha, \beta)$ transformation. A small difference observed in figure 5 is that this transformation occurred over a broad range of temperature up to 573 K on heating in the dilatometry experiment but was completed at 423 K in the x-ray experiment. This discrepancy is probably due to the different heating histories used in the two experiments: 2 K min^{-1} with 15 min holding times at 373, 473 and 573 K for the dilatometry experiment [1], as compared with rapid heating (about 60 K min^{-1}) with holding times of about 15 min at each temperature investigated in the present x-ray experiment. Also, the initial volume fraction of γ-phase may have been somewhat different in the two experiments. On cooling (see figure 5), the thermal contraction at high temperatures predicted by ROM and the Turner upper bound (equations (4) and (5)) bracket the measured value as expected. At high temperatures, plastic deformation of the copper matrix causes less elastic interaction between the ceramic and metal constituents of the composite. Thus ROM

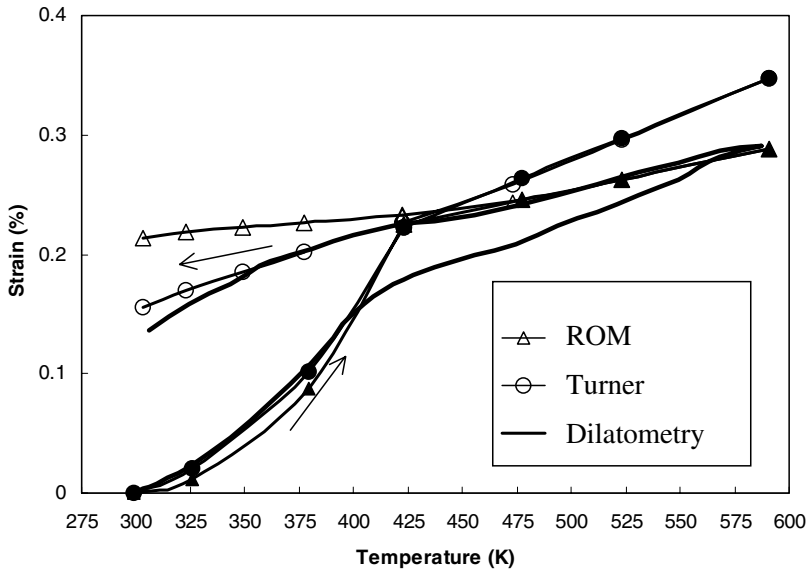

Figure 5. Temperature dependence of the thermal strain of Cu–ZrW_2O_8 composite as measured by dilatometry in [1] and as calculated from equations (4) and (5) with the phase volume fractions (figure 4).

Table 2. Bulk modulus K, shear modulus G and CTE α of individual phases used for the CTE calculations of Cu–ZrW_2O_8 composite.

Phase	K (GPa)	G (GPa)	CTE α (10^{-6} K^{-1})
Cu	138[a] [20]	42.1[a] [20]	16.7[b] [19]
α-ZrW_2O_8	72.5 [9]	33.4[c]	−13.5 [4] (298–428 K)
β-ZrW_2O_8	72.5 [9]	33.4[c]	−6.5 [4] (428–600 K)
γ-ZrW_2O_8	65.4 [9]	30.1[c]	1.6 [9] (300–390 K)

a With temperature dependence as given in [19].
b With temperature dependence as given in [20].
c Calculated from bulk modulus and Poisson ratio ($\nu = 0.3$) with isotropic assumption [21].

results are closer to measured values on cooling, at high temperatures (figure 5). Similarly, at low temperatures on cooling (figure 5), results of Turner's expression, which includes terms for elastic interaction, are closer to the dilatometry measurements. A somewhat higher contraction is observed by dilatometry below 348 K on cooling, which may again be due to a slightly larger formation of γ-phase due to the lower cooling rate. The above observations thus confirm that the highly variable and anomalously large CTE of the Cu–ZrW_2O_8 composite observed by Holzer and Dunand [1] is due to the reversible formation of γ-phase. Therefore, as suggested by these authors, inhibition of this transformation by reduction of mismatch stresses and/or alteration of the ZrW_2O_8 chemistry should result in composites with high thermal conductivity and low, uniform CTE (which could become zero or even negative with a higher ceramic content).

The overall agreement in figure 5 between the curves as experimentally measured by dilatometry and as calculated from volume fractions determined by x-rays is surprisingly good, given the experimental error on the volume fractions (predicted to be $\pm 8\%$ for γ-phase considering the errors of the measured intensities and of the initial volume fraction), the

range of possible models for the CTE of the ceramic and the composite and the uncertainties associated with the materials constants listed in table 2. By far the most sensitive parameter in the calculations is the ceramic CTE (equation (6)), which, in the temperature range where the γ-phase exists, is dominated by the value of $\Delta V/V$ (derived from precise unit-cell volume measurements by neutron diffraction [7, 9]) and the initial volume fraction of the γ-phase (derived from synchrotron x-ray measurements and controlling $\Delta V_\gamma/\Delta T$ in equation (6)). Also important in equation (6) are the magnitudes of thermal expansions for each of the ceramic phases taken from precise unit-cell volume measurements by neutron diffraction [4,9], which were considered to be more accurate than the dilatometric values measured on sintered ZrW_2O_8 samples [2].

6. Conclusions

Transmission diffraction patterns of a Cu–ZrW_2O_8 MMC were recorded as a function of temperature upon cycling between 298 and 591 K, using a high-energy, high-intensity x-ray synchrotron beam allowing for bulk phase measurement of a large volume of sample. The following main conclusions can be drawn.

(1) Polymorphic transformations of the ceramic between the low-pressure, cubic phases (α- and β-ZrW_2O_8) and the high-pressure orthorhombic phase (γ-ZrW_2O_8) were observed *in situ* by monitoring the intensity of the diffraction rings belonging to each phase.
(2) The volume fractions of the three ceramic phases were calculated using the intensity data as a function of temperature. The initial mixture of α- and γ-phases transforms on heating to the β-phase. On cooling, the reverse transformation occurs, but the γ-phase volume fraction at the end of the cycle is much lower than at the beginning.
(3) Good agreement was found for the thermal strain developed by the γ-ZrW_2O_8 component over the whole temperature cycle, as determined by dilatometry in an earlier investigation [1] and as calculated from the volume fraction of ceramic measured by x-ray diffraction in the present investigation. These direct measurements thus confirm the earlier hypothesis [1] based on dilatometry that the anomalously high thermal expansion/contraction of these composites is due to the volume change of the ceramic particle associated with polymorphic phase transformation to and from γ-ZrW_2O_8.

Acknowledgments

I am grateful to Professor D C Dunand (Northwestern University) who introduced me to the subject and offered me the opportunity of the experimental study and helpful discussions. The diffraction experiments were performed at the DuPont–Nortwestern–Dow Collaborative Access Team (DND-CAT) Synchrotron Research Center at the Advanced Photon Source (APS), whose staff I acknowledge for technical support.

References

[1] Holzer H and Dunand D C 1999 *J. Mater. Res.* **14** 780
[2] Martinek C and Hummel F A 1968 *J. Am. Ceram. Soc.* **51** 227
[3] Mary T A, Evans J S O, Vogt T and Sleight A W 1996 *Science* **272** 90
[4] Evans J S O, Mary T A, Vogt T, Subramanian M A and Sleight A W 1996 *Chem. Mater.* **8** 2809
[5] Pryde A K A, Hammonds K D, Dove M T, Heine V, Gale J D and Warren M C 1996 *J. Phys.: Condens. Matter* **8** 10 973
[6] Pryde A K A, Hammonds K D, Dove M T, Heine V, Gale J D and Warren M C 1997 *Phase Transitions* **61** 141

[7] Evans J S O, Hu Z, Jorgensen J D, Argyriou D N, Short S and Sleight A W 1997 *Science* **275** 61
[8] Hu Z, Jorgensen J D, Teslic S, Short S, Argyriou D N, Evans J S O and Sleight A W 1998 *Physica* B **241–3** 370
[9] Jorgensen J D, Hu Z, Teslic S, Argyriou D N, Short S, Evans J S O and Sleight A W 1999 *Phys. Rev.* **59** 215
[10] Sleight A W 1998 *Annu. Rev. Mater. Sci.* **28** 29
[11] von der Gonna J, Meurer H J, Nover G, Peun T, Schonbohm D and Will G 1998 *Mater. Lett.* **33** 321
[12] Yagi T, Akaogi M, Shimomura O, Suzuki T and Akimoto S 1987 *J. Geophys. Res.* **92** 6207
[13] Svensson S O, Vogl G, Kaisermary M and Kvick A 1997 *Acta Mater.* **45** 4205
[14] Kremenovic A, Norby P, Dimitrijevic R and Dondur V 1997 *Phase Transitions* **68** 587
[15] Kulkov S K and Mironov Y P 1995 *Nucl. Instrum. Methods Phys. Res.* A **359** 88
[16] Cullity B D 1978 *Elements of X-Ray Diffraction* (Menlo Park, CA: Addison-Wesley)
[17] Verdon C and Dunand D C 1997 *Scr. Mater.* **36** 1075
[18] Turner P S 1946 *J. Res. Natl Bur. Stand.* **37** 239
[19] *Metals Handbook: Properties and Selection: Nonferrous Alloys and Pure Metals* 1979 (Metals Park, OH: American Society for Metals)
[20] Frost H J and Ashby M F 1982 *Deformation-Mechanism Maps: the Plasticity and Creep of Metal and Ceramics* (Oxford: Pergamon)
[21] Meyers M A and Chawla K K 1984 *Mechanical Metallurgy Principles and Applications* (Englewood Cliffs, NJ: Prentice-Hall)